IAI
Journals.ASM.org

# Use of Recombinase-Based *In Vivo* Expression Technology To Characterize *Enterococcus faecalis* Gene Expression during Infection Identifies *In Vivo*-Expressed Antisense RNAs and Implicates the Protease Eep in Pathogenesis

**Kristi L. Frank, Aaron M. T. Barnes, Suzanne M. Grindle, Dawn A. Manias, Patrick M. Schlievert,* and Gary M. Dunny**

Department of Microbiology, University of Minnesota Medical School, Minneapolis, Minnesota, USA

***Enterococcus faecalis* is a member of the mammalian gastrointestinal microflora that has become a leading cause of nosocomial infections over the past several decades. *E. faecalis* must be able to adapt its physiology based on its surroundings in order to thrive in a mammalian host as both a commensal and a pathogen. We employed recombinase-based *in vivo* expression technology (RIVET) to identify promoters on the *E. faecalis* OG1RF chromosome that were specifically activated during the course of infection in a rabbit subdermal abscess model. The RIVET screen identified 249 putative *in vivo*-activated loci, over one-third of which are predicted to generate antisense transcripts. Three predicted antisense transcripts were detected in *in vitro*- and *in vivo*-grown cells, providing the first evidence of *in vivo*-expressed antisense RNAs in *E. faecalis*. Deletions in the *in vivo*-activated genes that encode glutamate 5-kinase (*proB* [EF0038]), the transcriptional regulator EbrA (*ebrA* [EF1809]), and the membrane metalloprotease Eep (*eep* [EF2380]) did not hinder biofilm formation in *in vitro* assays. In a rabbit model of endocarditis, the Δ*ebrA* strain was fully virulent, the Δ*proB* strain was slightly attenuated, and the Δ*eep* strain was severely attenuated. The Δ*eep* virulence defect could be complemented by the expression of the wild-type gene in *trans*. Microscopic analysis of early Δ*eep* biofilms revealed an abundance of small cellular aggregates that were not observed in wild-type biofilms. This work illustrates the use of a RIVET screen to provide information about the temporal activation of genes during infection, resulting in the identification and confirmation of a new virulence determinant in an important pathogen.**

Enterococci are both innocuous inhabitants of the human gastrointestinal tract and a leading cause of hospital-acquired infections. *Enterococcus faecalis* is responsible for the majority of enterococcal infections (38, 46), and the treatment or prevention of these infections can be complicated by the species' intrinsic and acquired mechanisms of resistance to numerous antibiotics as well as its ability to persist under harsh environmental conditions for extended periods of time (23). *E. faecalis* causes a wide variety of infections, including endocarditis, surgical-site infection, bacteremia, urinary tract infection, and endodontic infection (24). Previously reported *in vitro* studies provided evidence that many *E. faecalis* virulence genes are differentially expressed when grown in blood, serum, and urine (27, 53, 64), demonstrating that gene expression profiles change based on the microenvironment in which the organism is located. This characteristic is likely a key factor contributing to the pathogenesis of *E. faecalis* infections.

In order to thrive as a pathogen, *E. faecalis* must be able to colonize the site of infection, adapt to changes in nutrient availability, and evade phagocytes and other innate immune system defenses. Biofilm formation is a strategy frequently employed by pathogenic microbes to circumvent challenges posed by host environments, so it is not surprising that many *E. faecalis* infections have a biofilm etiology (37). Our laboratory previously used a two-pronged genetic approach involving transposon mutagenesis (31) and recombinase-based *in vivo* expression technology (RIVET) (4) to identify determinants of biofilm formation in the genome of *E. faecalis* OG1RF. This well-characterized laboratory strain lacks plasmids and many other mobile genetic elements that are typically present in clinical isolates such as V583 (7, 44), but it is still capable of forming biofilms and producing robust infections in experimental animals (7, 30). The conserved genetic determinants identified in this strain are likely part of the core genome shared by all *E. faecalis* strains and may be attractive targets for the development of vaccines or chemotherapeutic agents. Our previous screens revealed several dozen genes, many of which were not previously associated with biofilm development, that support *E. faecalis* biofilm growth under *in vitro* conditions. However, the extent to which these and most other biofilm-associated genes are used by *E. faecalis* during *in vivo* growth is unknown.

A number of methods have been used to study bacterial gene expression *in vivo*. Numerous *in vivo* microarray experiments, which assess bacterial transcription on a global scale, have been reported (26, 32, 41, 58, 61, 63, 66). Genetic techniques that facilitate genome-wide screening for specific *in vivo*-expressed genes include signature-tagged mutagenesis, which results in the identification of virulence genes among libraries of uniquely tagged transposon mutants, and *in vivo* expression technology (IVET),

**Received** 20 September 2011 **Returned for modification** 18 October 2011
**Accepted** 19 November 2011
**Published ahead of print** 5 December 2011
**Editor:** A. Camilli

Address correspondence to Kristi L. Frank, fran0616@umn.edu.
* Present address: Department of Microbiology, University of Iowa, Iowa City, Iowa, USA.

Supplemental material for this article may be found at http://iai.asm.org/.



doi:10.1128/IAI.05964-11

**TABLE 1** *Enterococcus faecalis* strains and oligonucleotides used in this study

| Strain or oligonucleotide | Description or sequence | Reference(s) |
|---|---|---|
| Strains | | |
| OG1RF | Wild-type strain | 21 |
| OG1RF Δ*proB* | Markerless in-frame deletion of locus EF0038 | This study |
| OG1RF Δ*ebrA* | Markerless in-frame deletion of locus EF1809 | 4; K. S. Ballering and G. M. Dunny, unpublished data |
| OG1RF Δ*eep* | Markerless in-frame deletion of locus EF2380; also called JRC106 | 29 |
| OG1RF Δ*eep*(pMSP3535-*eep*) | Complementation plasmid; *eep* ORF with RBS cloned under expression of nisin-inducible promoter[a] | This study |
| Oligonucleotides | | |
| NotI+0038F | 5′-CCCCGCGGCCGCCAAACTTACTCTAGCACGACGATC | This study |
| NcoI+0038R | 5′-CCCCCCATGGTTCAGAATGTTTTGTATTGTAGCGATT | This study |
| 0038-2stepF | 5′-AGAAACGAGGCACTTATGAGAAACAGTGACTGATTTAAAGCAACTAGGGC | This study |
| 0038-2stepR | 5′-GCCCTAGTTGCTTTAAATCAGTCACTGTTTCTCATAAGTGCCTCGTTTCT | This study |
| EF2380 XhoI F | 5′-CTAGTCTCGAGTTAAAAGAAAAAGCGTTGAATATCG | This study |
| EF2380 SpeI R RBS | 5′-CTAGTACTAGTGAATGAAGGAAGAAGGACATCTATG | This study |
| RIVET forward | 5′-AGCGTCGACTCTAGAGATCCAG | 4 |
| RIVET reverse | 5′-TACCCGTGCGTAACCAAAAAGTCG | 4 |
| EF0223F | 5′-TCACCGACAACAACTAAAGCT | This study |
| EF0223R | 5′-CATTTGGAATTAGAAGACCGC | This study |
| EF0909F | 5′-TAAGTTTTTCTTGGTTGGTATAAG | This study |
| EF0909R | 5′-ATCTTTTTCATGATTATCACTTTG | This study |
| EF2398F | 5′-GTTACCTTCGATGAAAGCGTC | This study |
| EF2398R | 5′-TCCTGATGAGATCGATGTTGT | This study |

[a] See reference 8.

which is a promoter-trapping strategy that identifies promoters activated during infection (15). RIVET is a variation of IVET that uses transcriptional fusions to drive the expression of a promoterless DNA recombinase, which mediates an irreversible and heritable recombination event that can be detected in screens or selections (10). RIVET has been used with a diverse range of pathogens, including *Vibrio cholerae* (11, 43), *Helicobacter pylori* (12), and *Staphylococcus aureus* (33), and offers the benefit of being able to identify transiently expressed *in vivo*-induced genes that exhibit various levels of transcription (56).

In order to understand the genetic mechanisms that enable *E. faecalis* to establish infection and persist within a host, we used RIVET to investigate gene activation during the onset of infection in a rabbit subdermal abscess model. The RIVET screen identified a large number of putative *in vivo*-activated promoters oriented in both the sense and antisense directions, suggesting a genome-wide upregulation of transcription during growth in a mammalian environment. Transcripts from three of the putative antisense promoters were experimentally confirmed *in vivo*. Three sense-orientation, *in vivo*-activated genes that were also identified by our previously reported RIVET screen for biofilm-activated genes (4) were characterized for biofilm formation using *in vitro* assays and a rabbit model of experimental endocarditis. Notably, we found that the membrane metalloprotease Eep has an aberrant cell distribution phenotype during early biofilm formation and is required for *E. faecalis* endocarditis.

## MATERIALS AND METHODS

**Bacterial strains, growth conditions, and chemicals.** *E. faecalis* strains used in this study are listed in Table 1. *E. faecalis* was routinely grown aerobically in brain heart infusion (BHI) broth (BD Bacto, Becton, Dickinson, and Company, Sparks, MD) or Todd-Hewitt broth (THB; BD Bacto) under static conditions, or on BHI agar, at 37°C. Cultures for animal experiments were grown in trypsinized beef heart dialysate (BH) medium (48) under static conditions at 37°C for OG1RF subdermal chamber inocula; at 30°C, except as noted below, for OG1RF RIVET strain subdermal chamber inocula (4); and at 37°C with 7% $CO_2$ for endocarditis inocula.

Lysozyme, mutanolysin, 5-fluorouracil (5FU), nisin, and all antibiotics were purchased from Sigma-Aldrich (St. Louis, MO). Stock solutions of 5FU at 50 mg/ml in dimethyl sulfoxide (DMSO) were prepared immediately before use. Stock solutions of other drugs were prepared as follows and stored at −20°C: nisin at 25 μg/ml in water, erythromycin at 50 mg/ml in methanol, chloramphenicol at 20 mg/ml in methanol, and kanamycin at 100 mg/ml in water. All restriction enzymes were purchased from New England BioLabs (Ipswich, MA). *Pfu* Ultra II Fusion DNA polymerase (Agilent Technologies, Santa Clara, CA) was used for all PCRs performed for strain and plasmid construction. Oligonucleotides were synthesized by Invitrogen (Carlsbad, CA) and are listed in Table 1.

**Strain and plasmid construction.** The OG1RF Δ*proB* (locus EF0038) strain was constructed by using a previously described allelic exchange method (29). The deletion construct used for allelic exchange was generated with overlap-extension PCR by first amplifying two ~1-kb fragments from OG1RF genomic DNA with primer pairs 0038-2stepR and NotI+0038F and NcoI+0038R and 0038-2stepF. The two products were annealed together, and second-step amplification was performed with primers NotI+0038F and NcoI+0038R. The resulting product was digested with NotI and NcoI, ligated into pCJK47 (29) predigested with the same enzymes, and propagated in *Escherichia coli* EC1000 cells grown on BHI medium with 100 μg/ml erythromycin. The deletion of *proB* had no effect on growth (data not shown).

Plasmid pMSP3535-*eep* was constructed by PCR amplification of the *eep* (locus EF2380) open reading frame (ORF) from OG1RF genomic DNA with primers EF2380 XhoI F and EF2380 SpeI R RBS. The resulting product was digested with XhoI and SpeI, ligated into pMSP3535 (8)

predigested with the same enzymes, and propagated in *E. coli* DH5α or *E. faecalis* OG1RF Δ*eep* cells grown on BHI medium with 75 μg/ml or 10 μg/ml erythromycin, respectively. There were no differences in the growth rates of OG1RF, the OG1RF Δ*eep* strain, or the OG1RF Δ*eep*(pMSP3535-*eep*) strain (data not shown).

**Rabbit models of subdermal abscess infection and endocarditis.** All animal procedures were carried out in accordance with the guidelines set forth by the Public Health Service Policy on Humane Care and Use of Laboratory Animals. The University of Minnesota Institutional Animal Care and Use Committee approved the protocol used in this work (approval number 0910A73332). Animals were euthanized with Beuthanasia-D, and efforts were made to minimize suffering.

Subdermal chambers were implanted into the flanks of New Zealand White rabbits (male or female, 2 to 3 kg) essentially as previously described (50, 60). Briefly, hollow perforated polyethylene golf balls were obtained from a sporting goods store and were sterilized by boiling in phosphate-buffered saline (PBS) for 30 min. After cooling, a single chamber was aseptically placed through an incision into a surgically created subcutaneous pocket in each anesthetized rabbit. Incisions were sutured closed, and animals were allowed to heal for at least 6 weeks before infection, during which time the chambers became encapsulated with fibrous tissue and filled with approximately 30 ml of serous fluid. Samples for RIVET analysis were obtained from two rabbits in which chambers had been implanted 10 and 28 weeks prior to infection. To initiate infection, 2 ml of serous fluid was aspirated from the subdermal chamber and was replaced with 2 ml of inoculum prepared as described below.

Endocarditis infections were carried out as previously described (16). Briefly, single colonies of each strain were inoculated into BH medium and grown overnight. Cultures of the OG1RF Δ*eep*(pMSP3535-*eep*) strain also contained 10 μg/ml erythromycin and 25 ng/ml nisin. Cells were pelleted and resuspended to an optical density at 600 nm of 1.0 in potassium phosphate-buffered saline (KPBS), corresponding to approximately $2 \times 10^9$ to $4 \times 10^9$ CFU/ml. Following surgery, 2 ml was administered intravenously via the marginal ear vein to initiate infection. Rabbits were euthanized after 4 days, at which point the hearts were removed and dissected to expose the aortic valve. Vegetations—the classic lesions associated with infectious endocarditis—and valve leaflets were harvested, weighed, homogenized in 1 ml of THB, serially diluted, and plated onto BHI agar to quantify bacteria. Homogenates from animals infected with the OG1RF Δ*eep*(pMSP3535-*eep*) strain were also plated onto BHI agar containing 10 μg/ml erythromycin to determine the percentage of cells that retained the complementation vector for the duration of the infection.

Endocarditis results were analyzed for statistical significance with the Wilcoxon rank-sum test with $\chi^2$ approximation using JMP software (version 8.0.2; SAS Institute, Inc., Cary, NC).

**RIVET screen in subdermal abscess infection.** The *E. faecalis* RIVET system, including the genomic library used in this study, was described previously (4). Aliquots of the library were grown for 5.5 to 6.5 h in 10 ml BH medium containing 2,000 μg/ml kanamycin and 10 μg/ml chloramphenicol ($BH_{kan2000cm10}$) and then diluted 1:20 into 10 to 25 ml of $BH_{kan2000cm10}$ and further incubated for 14 to 15.5 h. The cultures were diluted 1:5 into 50 ml $BH_{kan2000cm10}$ (rabbit A) or 100 ml BH medium without antibiotics (rabbit B) and incubated for 3 h at 30°C (rabbit A) or 2 h at 37°C (rabbit B). Bacteria were centrifuged for 15 min at 4,000 × *g* at 4°C and resuspended in KPBS to densities of ~$1 \times 10^7$ CFU/ml for rabbit A and ~$4 \times 10^9$ CFU/ml for rabbit B. Two-milliliter volumes were used for subdermal chamber infections. Approximately 1.5-ml aspirates were collected at 2, 4, 8, 24, and 96 h postinoculation from the chamber in rabbit A. For rabbit B, 4-ml aspirates were collected from the chamber at 2, 4, and 8 h postinoculation. Rabbit B was euthanized at 24 h and the chamber was retrieved. The explanted chamber was bisected, and the interior surfaces were scraped several times with a sterile rubber policeman that was repeatedly rinsed in a tube containing 25 ml KPBS. Six tissue sections that appeared to contain white abscesses formed at the sites of chamber perforations were harvested, rinsed with 1 ml KPBS, and homogenized in 2 ml KPBS. Aliquots of the initial inocula and all collected samples were plated onto BHI agar with and without 20 μg/ml chloramphenicol to determine the bacterial load and to assess whether the RIVET library plasmid was lost from cells during infection due to the lack of antibiotic selection in chambers. Cell counts indicated that the plasmid was lost at a low, but variable, frequency starting at 4 to 8 h postinoculation (data not shown). Bacterial counts reported in Fig. 1 are from chloramphenicol plates, in order to represent the number of cells containing the RIVET plasmid at each time point assayed.

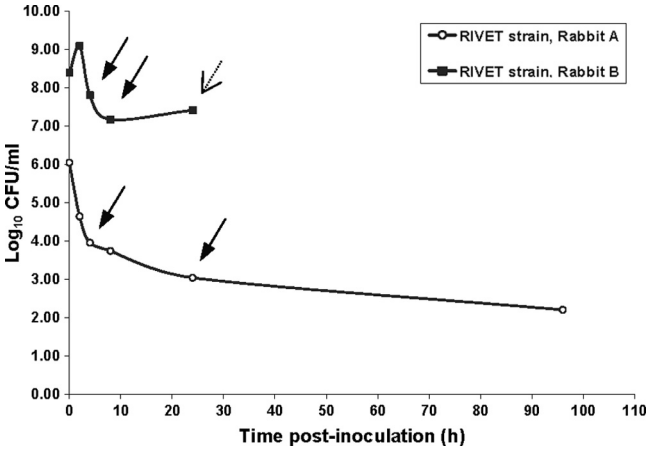


**FIG 1** Recovery of the *E. faecalis* RIVET strain from subdermal abscesses. Two milliliters of the *E. faecalis* OG1RF RIVET library was inoculated into subdermal chambers from which 2 ml of serous fluid was withdrawn. Dilutions of fluid aspirated from implanted chambers at the indicated time points following inoculation were plated to determine the number of viable *E. faecalis* CFU recovered. Results are reported as $\log_{10}$ CFU/ml. The 0-h time points were calculated by dividing the total CFU in the 2-ml inocula by 30 ml, the volume of serous fluid in the implanted chamber. Arrows indicate the time points analyzed by RIVET: 4, 8, and 24 h postinoculation. Infection of rabbit A was carried out for 96 h, whereas infection of rabbit B was terminated at 24 h, at which time the chamber was explanted and samples were harvested from the chamber surface and surrounding tissues (open-head arrow).

**Analysis of RIVET clones for *in vivo*-activated promoters.** RIVET clones that underwent a chromosomal excision event were selected by plating on BHI agar containing 20 μg/ml chloramphenicol and 130 μg/ml 5FU. Individual colonies were patched onto BHI agar containing 20 μg/ml chloramphenicol, 130 μg/ml 5FU, and 1,000 μg/ml kanamycin. All chloramphenicol- and 5FU-resistant, kanamycin-sensitive colonies were grown overnight in 5 to 10 ml BHI medium with 20 μg/ml chloramphenicol and treated with 30 mg/ml lysozyme in 0.4 ml TE (100 mM Tris-HCl [pH 8], 1 mM EDTA) for 30 to 45 min at 37°C. RIVET plasmids were harvested from lysozyme-treated cells with the QIAprep Spin miniprep kit (Qiagen, Inc., Valencia, CA). Plasmid inserts were sequenced at the University of Minnesota BioMedical Genomics Center DNA Sequencing and Analysis Facility with primers RIVET forward and RIVET reverse (4). Sequences were aligned by using Sequencher software (version 4.9 or earlier; Gene Codes Corp., Ann Arbor, MI) and then BLASTed against the *E. faecalis* V583 genome at the J. Craig Venter Institute (JCVI) Comprehensive Microbial Resource to identify the ORF downstream of the putative promoter. When the RIVET insert spanned more than one ORF, particularly when adjacent ORFs were separated by a sizable intergenic region, the putative *in vivo*-activated promoter was assigned to the furthest downstream ORF. In contrast, when two or more ORFs were directly adjacent or overlapping, thus appearing that they are likely to be cotranscribed, the putative promoter was assigned to the first ORF in the group. Sequences containing OG1RF-specific regions were initially compared to the NCBI GenBank *E. faecalis* OG1RF genome (accession number ABPI00000000.1) (7), but because the annotation of that sequence re-

mained incomplete until recently (updated in 2011 with accession number CP002621), ORF identifications were obtained by using an OG1RF annotation generated with the Rapid Annotation Using Subsystem Technology (RAST) server (3) (see Table S1 and supplemental materials and methods in the supplemental material).

**Gene expression analysis of antisense transcripts in OG1RF from the subdermal abscess model.** Subdermal abscess infections with *E. faecalis* OG1RF were carried out with three rabbits, as described above. A single colony of *E. faecalis* OG1RF was inoculated into 10 to 25 ml of BH medium, incubated for approximately 15 h, diluted 1:5 into 25 to 50 ml of fresh BH medium, and incubated for two more hours. Bacteria were centrifuged for 15 to 20 min at 2,250 × *g* at 4°C. Pelleted cells were resuspended to an optical density at 600 nm of ~1.3 to 1.6 in KPBS, and 2 ml was used for each subdermal chamber infection. Approximately 2 ml of the initial inoculum and chamber aspirates harvested at 4 h postinoculation were immediately added to 4 ml of RNAprotect Bacteria reagent (Qiagen, Inc.), processed according to the manufacturer's instructions, flash-frozen, and stored at −80°C until RNA extraction.

Frozen aspirates were thawed, resuspended in 0.4 ml of RNase-free TE containing 50 mg/ml lysozyme and 1,000 U/ml mutanolysin, homogenized with a hand-held motorized pestle, and incubated for 10 min at 37°C. Each sample was then split in half and extracted in duplicate with the RNeasy minikit (Qiagen, Inc.) according to the manufacturer's instructions, with an added QIAshredder (Qiagen, Inc.) homogenization step immediately after the addition of buffer RLT. RNA was eluted from each column with two 30-μl volumes of RNase-free water, and total RNAs from duplicate extractions of each sample were pooled together. Contaminating DNA was removed by using a Turbo DNA-free kit (Ambion, Austin, TX) according to the rigorous protocol provided by the manufacturer. cDNA was synthesized with gene-specific primers using the SuperScript III first-strand synthesis system for reverse transcription (RT)-PCR (Invitrogen Corp.). Quantitative PCR (qPCR) was carried out with an iQ5 iCycler real-time detection system (Bio-Rad Laboratories, Inc., Hercules, CA) with iQ SYBR green Supermix (Bio-Rad Laboratories, Inc.). Each reaction was performed in triplicate, and threshold cycle ($C_T$) values were averaged. EF0886, which was identified by microarray analysis as being a gene with nonchanging expression at the analyzed time points (K. L. Frank and G. M. Dunny, unpublished data), was used as a reference gene. The fold change for each sample was calculated according to a method described previously by Pfaffl (45), and the three biological replicates were averaged together to obtain the reported fold change.

**Biofilm microscopy.** *E. faecalis* biofilms were grown on 11-mm-diameter Aclar fluoropolymer coupons (Aclar embedding film, 7.8-mil thickness; Electron Microscopy Sciences, Hatfield, PA) in tryptic soy broth without added dextrose ($TSB_{-dex}$; Becton, Dickinson, and Company) under gentle agitation (150 rpm) for 6 h. After washing three times with PBS, the cell envelope was labeled by using a red fluorescent wheat germ agglutinin (WGA)-Alexa Fluor 594 conjugate (Invitrogen), and the coupons were mounted in Vectashield HardSet medium (Vector Laboratories, Burlingame, CA). Images were acquired with a Cascade 1k electron-multiplying charge-coupled device camera (Photometrics, Tucson, AZ) as wide-field *z* stacks with a 20× 0.75-numerical-aperture (NA) or a 60× 1.4-NA objective (Nikon Instruments, Melville, NY). Images of *z* stacks were taken at 0.4- or 0.15-μm intervals (20× and 60×, respectively) and deconvolved using Huygens Professional software (version 3.7.1; Scientific Volume Imaging, Netherlands). The presented images are maximum intensity projections determined by using ImageJ (version 1.5k; NIH, Bethesda, MD) and are representative of at least three biological and four technical replicates per sample. The COMSTAT2 software package was used to quantify biofilm biomass (28).

## RESULTS

**RIVET screen to identify promoters activated during subdermal abscess infection.** To explore *E. faecalis* gene activation *in vivo*, we used a subdermal chamber infection model that is amenable to time course sampling for the study of gene expression using genetic analysis or transcription profiling (67). This model consists of a subcutaneously implanted, hollow chamber with a perforated surface that becomes encapsulated after insertion, fills with a serous fluid containing immune cells, and mimics the environment of a localized abscess upon the introduction of bacteria (52, 60). *E. faecalis* cells remain localized within the chamber fluid, which initially contains a stable population of leukocytes comprised of ~10% polymorphonuclear cells and 90% mononuclear cells (60), while additional immune cells enter the chamber during the course of infection, thus exposing the bacteria to a changing host response.

Two independent RIVET screens were conducted with the same library used for our group's previous RIVET screen for *in vitro* biofilm formation genes (4). In this system, *in vivo*-activated promoters drive the expression of the gene for the site-specific recombinase TnpR. TnpR acts at its target sequences (*res* sites) to excise an engineered region of the chromosome in the RIVET strain that encodes genes for both kanamycin resistance and sensitivity to 5FU (*upp*); the latter serves as a counterselectable marker. Excision events result in a selectable and heritable change in genotype, as cells that have undergone resolution are rendered sensitive to kanamycin and resistant to 5FU (see Materials and Methods) (4). In order to eliminate promoters expressed constitutively or during growth in culture medium, the RIVET library inoculum was pregrown with high levels of kanamycin to select against *in vitro* resolution events.

The initial infection (rabbit A) (Fig. 1) represented the first use of our RIVET system *in vivo*. The RIVET library was inoculated at 6.0 $\log_{10}$ CFU/ml and was sampled at 2, 4, 8, 24, and 96 h postinoculation to assess survival. Bacterial counts dropped 2 logs during the first 4 h of infection, with a subsequent 1-log drop after 24 h. The strain persisted in the subdermal chamber for the duration of the 4-day infection. Clones were collected from chamber aspirates at 4 and 24 h postinoculation for screening, as we reasoned that these time points would allow sufficient time for cells to undergo resolution events following initial adaptation to the *in vivo* growth environment (4 h) and the activated host immune response (24 h). Dilutions of subdermal chamber fluid were plated onto counterselective medium containing 5FU to identify cells that underwent resolution. 5FU-resistant colonies were then tested for kanamycin sensitivity to confirm complete resolution.

Forty-six clones with the resolution phenotype were identified from 100 colonies screened from the 4-h aspirate. Only 38 clones with the correct phenotype were obtained after screening 1,550 colonies from the 24-h aspirate. The genomic DNA inserts from the 84 resolved clones were sequenced. The low rate of recovery of clones with the desired phenotype at 24 h (2.5%, compared to 46% at 4 h) suggested that selective pressures in the subdermal chamber environment caused genetic changes that resulted in high levels of background growth on the counterselection medium. For the subsequent infection (rabbit B), we focused on the 4- and 8-h time points rather than the 24-h time point.

A higher inoculum of ~8.5 $\log_{10}$ CFU/ml was used for the second infection (rabbit B) (Fig. 1). In contrast to RIVET rabbit A, the bacterial counts in RIVET rabbit B increased slightly at 2 h before dropping almost 2 logs to a low point at 8 h. Cell counts increased slightly by 24 h, at which time the experiment was terminated and the subdermal chamber was explanted in order to sample biofilm-associated *E. faecalis* cells from the inner surface of

the chamber. The inside of the tissue capsule from which the chamber was excised contained several small white pockets resembling abscesses at the regions corresponding to the perforations in the subdermal chamber; six of these tissue sections were also harvested, homogenized, and screened for resolved clones. Approximately 14% of colonies screened from the 4- and 8-h aspirates had the desired phenotype. In total, 133 clones from the 4-h aspirate, 163 clones from the 8-h aspirate, 57 clones from the chamber surface, and 99 clones from the tissues were found to have the correct phenotype and were sequenced for the second subdermal RIVET infection.

The combined sequencing of 536 clones from the two rabbits resulted in the identification of 249 unique upregulated loci from 260 nonsibling clones (see Tables S2 and S3 in the supplemental material). Forty-one of the unique upregulated loci were identified in rabbit A clones; 24.4% (10/41) of those loci were also identified among rabbit B clones. Eleven loci were identified by two unique clones spanning the same genomic region. Many of the nonunique clones were siblings of clones identified at earlier time points. Some inserts contained two nonadjacent genomic sequences, which are thought to represent library cloning artifacts, while a few sequenced plasmids contained no genomic inserts and were thus false positives, which further suggested that selective pressures in the subdermal chambers caused some degree of genetic rearrangements or deletions in the RIVET plasmid. Clones in the two latter categories were disregarded in the final analysis.

The RIVET clones fit into one of four categories with respect to orientation. The majority of the loci ($n = 114$) were identified by clones that contained a genomic sequence that overlapped at least one ORF and the associated 5′-untranslated region, which was assumed to contain the putative *in vivo*-activated promoter, in the same orientation (i.e., sense direction) as that of the recombinase (see Table S2 in the supplemental material). Forty-two loci were identified by sense-direction clones with genomic sequences that were located within an ORF, which indicates that internal promoters may be present (Table S2). The remaining 93 loci were identified from clones with genomic inserts whose directionality was oriented opposite that of the recombinase (i.e., antisense) (Table S3). Sixty-four of these loci overlapped one or more ORFs on the opposite DNA strand, whereas 29 were contained wholly within an ORF on the opposite DNA strand.

All but three of the identified loci contain protein-encoding ORFs; the other three loci encode large- and small-subunit rRNA genes. No clear patterns emerged among the protein-encoding loci when their predicted functions were considered by time point or source; therefore, RIVET clones were grouped according to their sense or antisense orientations in order to assess the distribution of functional categories represented among the putative *in vivo*-activated loci (Fig. 2). Approximately one-third of both the sense and antisense loci encode proteins with hypothetical or unknown functions. Many of the putatively activated genes identified in the RIVET screen have functions pertinent to cell growth and metabolism. Aside from the hypothetical proteins, transport and binding proteins comprised the largest functional category of sense clones (Fig. 2A). Interestingly, the same category was underrepresented among the antisense clones (Fig. 2B); conversely, more antisense than sense clones were present in the protein synthesis category.

**Identification of antisense RNAs expressed during mammalian infection.** Since more than one-third of the RIVET clones isolated were in an antisense orientation, we performed reverse transcription with gene-specific primers for selected putative antisense transcripts using RNA from OG1RF cells harvested from subdermal chamber inocula and from subdermal chamber aspirates at 4 h postinfection. We looked for the expressions of three antisense transcripts represented by RIVET antisense clones EF0226/0225/0224, EF0909, and EF2397/2398 (Fig. 3). These antisense RIVET clones were chosen from among more than 20

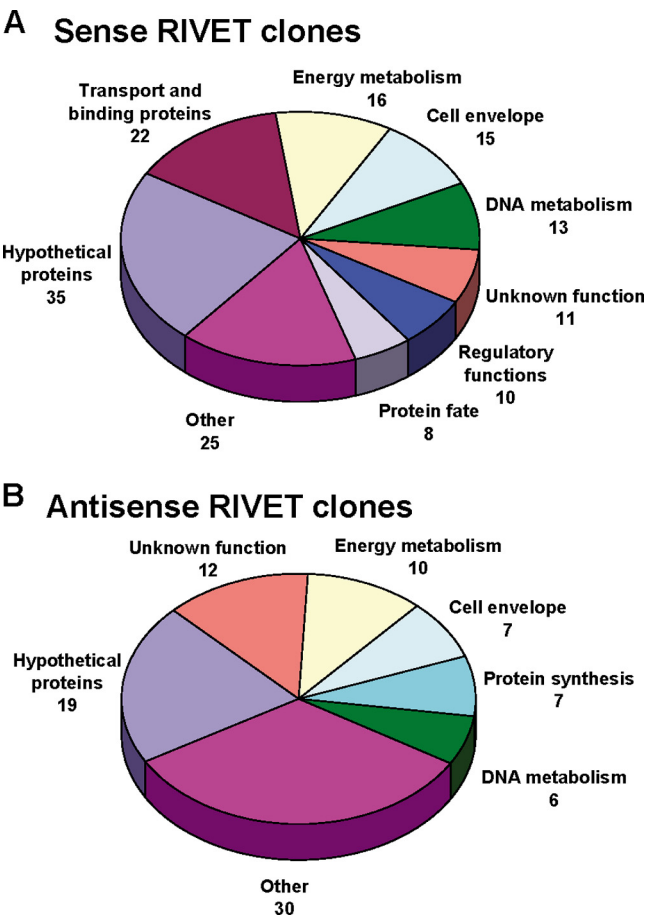


**FIG 2** Distribution of *E. faecalis* OG1RF sense (A) and antisense (B) RIVET clones isolated from a subdermal abscess infection. The *E. faecalis* genomic DNA sequence from each isolated RIVET clone was analyzed as described in Materials and Methods to determine the identity of the putative *in vivo*-activated promoter and the corresponding gene immediately downstream of the putative promoter. Each corresponding gene was assigned to a functional category by using the JCVI Comprehensive Microbial Resource (http://cmr.jcvi.org/tigr-scripts/CMR/CmrHomePage.cgi) for the *E. faecalis* V583 genome. All protein-encoding loci, as listed in Tables S2 and S3 in the supplemental material, were included. The number of genes in each functional category is given. The functional categories classified as "other" in panel A are as follows: cellular processes (5 genes); fatty acid and phospholipid metabolism (4 genes); pyrimidines, nucleosides, and nucleotides (4 genes); protein synthesis (4 genes); amino acid biosynthesis (2 genes); signal transduction (2 genes); transcription (2 genes); biosynthesis of cofactors, prosthetic groups, and carriers (1 gene); and mobile and extrachromosomal element functions (1 gene). The functional categories classified as "other" in panel B are as follows: biosynthesis of cofactors, prosthetic groups, and carriers (5 genes); pyrimidines, nucleosides, and nucleotides (5 genes); regulatory functions (5 genes); signal transduction (4 genes); cellular processes (3 genes); transport and binding proteins (3 genes); central intermediary metabolism (2 genes); fatty acid and phospholipid metabolism (1 gene); protein fate (1 gene); and transcription (1 gene).

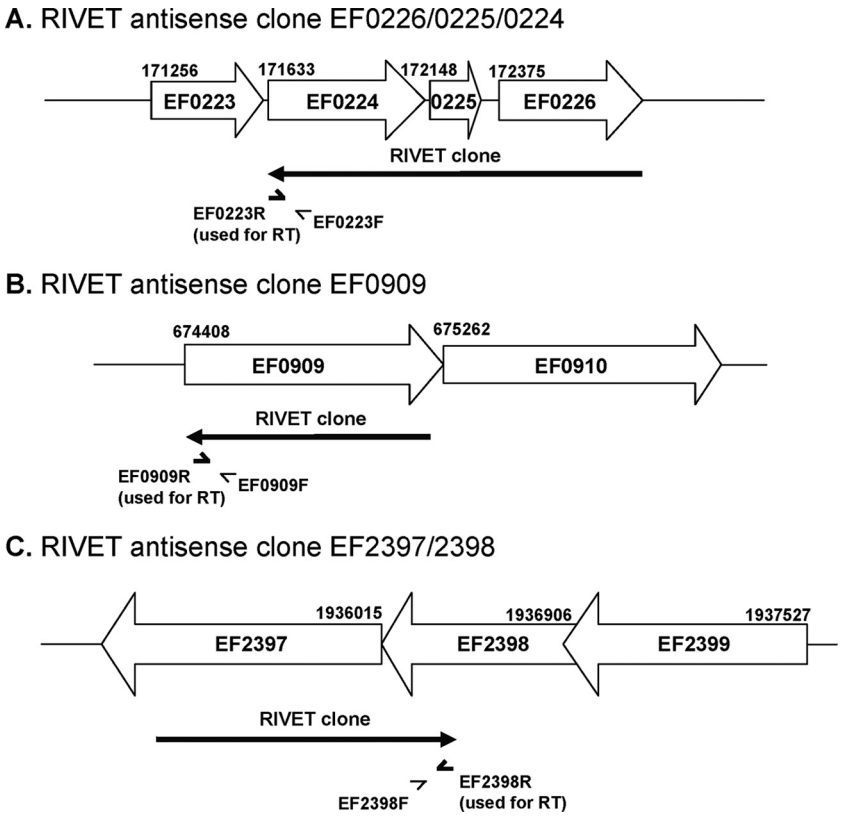


**FIG 3** Orientation of antisense RIVET clones and location of detected antisense transcripts. (A) RIVET antisense clone EF0226/0225/0224. (B) RIVET antisense clone EF0909. (C) RIVET antisense clone EF2397/2398. The genomic orientations of three antisense RIVET clones (black arrows) that predicted the presence of antisense transcripts are shown. The relative locations of primers used to subsequently detect and quantify the antisense transcripts by quantitative RT-PCR are indicated by heavy (reverse primers, used for reverse transcription and amplification) and light (forward primers, used for amplification) half-arrows. The nucleotide start site of each ORF, as annotated in Table S1 in the supplemental material, is indicated at its 5′ end. Although the graphic is not drawn to scale, the arrows representing adjacent genes within a locus are proportional to one another.

unique RIVET clones that each correlated with a cognate sense-strand gene that was found by microarray analysis to be significantly downregulated at 8 h in the subdermal abscess model (Frank and Dunny, unpublished).

We succeeded in amplifying all three transcripts from OG1RF cells grown *in vitro* and *in vivo*, whereas no signal was detected in any of the no-reverse-transcriptase controls (data not shown). Quantitative RT-PCR of the *in vivo*-expressed antisense RNAs revealed that the transcripts identified by antisense RIVET clones EF2397/2398 and EF0909 were upregulated at 4 h by 1.5-fold (standard deviation, 1.1) and 1.4-fold (standard deviation, 1.4), respectively ($n = 3$ each). This is consistent with the RIVET screen in that the EF2397/2398 and EF0909 antisense clones were identified at 4 h. The antisense RNA identified by antisense RIVET clone EF0226/0225/0224 was downregulated *in vivo* at 4 h by 1.7-fold (standard deviation, 0.6; $n = 3$). The EF0226/0225/0224 antisense RIVET clone was identified in tissue harvested from the subdermal abscess infection site at 24 h postinfection, suggesting that this transcript is transiently upregulated at some point during infection other than at 4 h or that it was expressed in a subpopulation of cells in the host; the same considerations may also be relevant to the relatively low levels of upregulation measured for the other two antisense transcripts. The primary significance of these results is that the existence of novel putative transcripts expressed *in vivo*, which were suggested by the RIVET screen, is supported by the RT-PCR experiments. This will allow for subsequent precise identification of the relevant antisense promoters, time course studies of antisense promoter expression, and functional studies of the effects of the antisense transcripts on the expression of mRNAs generated from the respective cognate sense strands.

**Identification of *in vivo*-activated genes also associated with biofilm growth *in vitro*.** We compared the *in vivo*-activated sense genes from the subdermal abscess RIVET screen (see Table S2 in the supplemental material) with the genes identified in previous transposon and RIVET screens for determinants of biofilm formation (4, 31). In total, 28 genes from the subdermal abscess RIVET screen were identified in the biofilm formation genetic screens (Table 2). Only two of the putative *in vivo*-activated promoters overlapped with the *in vitro* biofilm mutants found in the transposon screen, while the other 26 genes overlapped with promoters isolated from *in vitro* biofilm RIVET clones. Five of the genes are functionally annotated as transporters, and four genes have roles in energy metabolism. Two transcriptional regulators were also upregulated in biofilms and *in vivo*.

**Role of *in vivo*-activated genes in endocarditis.** We hypothesized that genes found in both the *in vivo* and biofilm RIVET screens (Table 2) may be important for biofilm formation in the host. To evaluate this possibility, we tested strains with markerless in-frame deletions of three genes listed in Table 2—*proB* (EF0038), encoding glutamate 5-kinase; *ebrA* (EF1809), encoding a transcriptional regulator; and *eep* (EF2380), encoding a membrane metalloprotease—in

**TABLE 2** *E. faecalis* OG1RF loci identified by an *in vivo* RIVET screen which were also identified by previously reported RIVET[e] or transposon[f] screens for *in vitro* biofilm formation

| Locus | Gene description | JCVI functional category | Time(s) postinoculation (h) or location of isolation of *in vivo* RIVET clone[a] | Time(s) of isolation of *in vitro* biofilm RIVET clone[b] | Transposon insertion mutant defective in *in vitro* biofilm formation[c] |
|---|---|---|---|---|---|
| EF0038 | Glutamate 5-kinase | Amino acid biosynthesis | 4 | 5 days | |
| EF0059 | UDP-*N*-Acetylglucosamine pyrophosphorylase | Cell envelope | 4 | 2 h, 3 days, 5 days | |
| EF0082 | Major facilitator family transporter | Transport and binding proteins | 4 | 2 h | |
| EF0246 | Amino acid ABC transporter, ATP-binding protein | Transport and binding proteins | 4 | 2 h, 5 days | |
| EF0402 | $Na^+/H^+$ antiporter | Transport and binding proteins | 4 | 2 h | |
| EF0721 | ATP-dependent DNA helicase PcrA | DNA metabolism | 8 | | + |
| EF0722 | DNA ligase, NAD dependent | DNA metabolism | 24 | 5 days | |
| EF0798 | Hypothetical protein | Hypothetical proteins | 8 | 2 h, 3 days, 5 days | |
| EF1348 | Glucan 1,6-alpha-glucosidase, putative | Energy metabolism | 8 | 3 days | |
| EF1591 | Transcriptional regulator, AraC family | Regulatory functions | Tissue | 2 h, 3 days | |
| EF1755 | Phosphate ABC transporter, ATP-binding protein | Transport and binding proteins | 4 | 3 days, 5 days | |
| EF1809 | Transcriptional regulator, GntR family | Regulatory functions | Tissue | 3 days, 5 days | |
| EF1826 | Alcohol dehydrogenase, zinc containing | Energy metabolism | 4 | 3 days, 5 days | |
| EF1918 | Conserved hypothetical protein | Hypothetical proteins | 4 | 2 h, 3 days, 5 days | |
| EF1962 | Triosephosphate isomerase | Energy metabolism | 4 | 5 days | |
| EF1978 | DNA-3-methyladenine glycosylase | DNA metabolism | 4 | 2 h, 5 days | |
| EF2207 | DNA-binding protein, Fis family | Regulatory functions | 8 | 2 h, 5 days | |
| EF2380 | Membrane-associated zinc metalloprotease, putative | Protein fate | 8 | 5 days | |
| EF2570 | Aldehyde oxidoreductase, putative | Unknown function | 4, 24 | 3 days, 5 days | |
| EF2668 | Magnesium transporter | Transport and binding proteins | 8 | 3 days, 5 days | |
| EF2744 | Peptidase, M42 family | Protein fate | 8 | 2h, 3 days, 5 days | |
| EF2889 | 2-Hydroxy-3-oxopropionate reductase | Energy metabolism | 4 | 2 h | |
| EF3008 | Conserved hypothetical protein | Hypothetical proteins | Tissue | 5 days | |
| EF3056 | Sortase family protein | Cell envelope | 8 | | + |
| EF3124 | Polypeptide deformylase, authentic frameshift | Protein fate | Chamber surface | 5 days | |
| EF3177 | Conserved hypothetical protein | Hypothetical proteins | Tissue | 2h, 5 days | |
| EF3258 | Conserved hypothetical protein | Hypothetical proteins | 4 | 3 days, 5 days | |
| OG1RF0176 (EF2352)[d] | GTP-binding protein LepA | Unknown function | 4 | 2 h | |

[a] Indicates the sampling time or location from which the clone was isolated. Two nonsibling clones were isolated for EF2570 at the indicated time points. Tissue and chamber surface clones were isolated from a chamber explanted at 24 h postinoculation.

[b] Indicates time points when clones were isolated from *in vitro* biofilms (4).

[c] + indicates that a transposon insertion mutant defective in *in vitro* biofilm formation was obtained in the locus (31).

[d] Locus EF2352 is annotated as OG1RF0176 in *E. faecalis* OG1RF (7).

[e] See reference 4.

[f] See reference 31.

a rabbit model of endocarditis, which is a biofilm infection of the endocardium, including the heart valves. The *ebrA* gene was chosen because an Δ*ebrA* strain was previously shown to have a defect in the formation of biofilms on cellulose membranes (4). The *proB* gene was selected due to studies examining the contribution of proline to the survival and pathogenicity of other Gram-positive bacteria in select animal models (5, 51, 57). The *eep* locus was of particular interest because of its previously characterized function in the processing of peptide pheromone signals for conjugative plasmids (2, 13). The roles of the *proB* and *eep* loci in biofilm formation have not been studied previously for *E. faecalis*.

OG1RF infected injured aortic valves with a mean valve bacterial load of 7.4 $\log_{10}$ CFU (Fig. 4) and produced large vegetations (Table 3). Compared to OG1RF, the Δ*ebrA* strain was not impaired in either valve colonization or vegetation formation (Fig. 4 and Table 3), whereas the Δ*proB* strain exhibited a 2.3-$\log_{10}$ decrease in the valve bacterial load, which was statistically significant (Fig. 4). The Δ*eep* strain was severely attenuated in causing endocarditis, as evidenced by the 4-$\log_{10}$ decrease in numbers of CFU recovered from the heart valves of Δ*eep* strain-infected rabbits (Fig. 4). The significant defect was also readily apparent in the small vegetations observed for the mutant strain (Table 3).

**Complementation of the Δ*eep* strain rescues the endocarditis attenuation phenotype.** Upon observing the striking attenua-

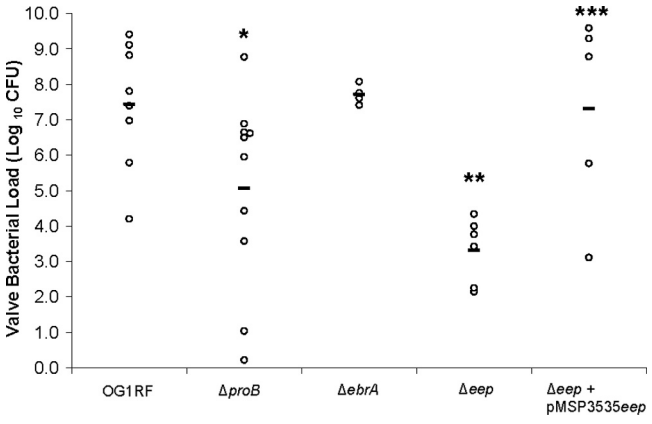


**FIG 4** Role of *in vivo*-activated, biofilm growth-associated genes in endocarditis virulence. A total of $10^9$ CFU of each *E. faecalis* strain was intravenously injected into New Zealand White rabbits following the induction of aortic valve damage, as described in Materials and Methods. Vegetations and heart valve leaflets were harvested at 4 days postinoculation. The $\log_{10}$ valve bacterial load is shown for wild-type strain OG1RF ($n = 8$), the OG1RF Δ*proB* strain ($n = 10$), the OG1RF Δ*ebrA* strain ($n = 4$), the OG1RF Δ*eep* strain ($n = 6$), and the OG1RF Δ*eep*(pMSP3535-*eep*) strain ($n = 5$). Horizontal bars denote the arithmetic means of the $\log_{10}$-transformed values. *, $P = 0.0367$ for OG1RF versus the Δ*proB* strain; **, $P = 0.003$ for OG1RF versus the Δ*eep* strain; ***, $P = 0.0446$ for the Δ*eep* strain versus the Δ*eep*(pMSP3535-*eep*) strain.

**TABLE 3** Weights of endocarditis vegetations produced by *E. faecalis* strains after 4 days of infection

| Strain | No. of vegetations | Mean vegetation wt (mg) | SD | *P* value |
|---|---|---|---|---|
| OG1RF | 8 | 47.6 | 29 | |
| Δ*proB* | 10 | 24.0 | 27.7 | 0.33[a] |
| Δ*ebrA* | 4 | 42.5 | 20.6 | 0.8651[a] |
| Δ*eep* | 6 | 8.8 | 6.6 | 0.0065[a] |
| OG1RF Δ*eep*(pMSP3535-*eep*) | 5 | 32.1 | 35.3 | 0.027[b] |

[a] Compared to OG1RF.
[b] Compared to the Δ*eep* strain

tion of the Δ*eep* strain in the endocarditis model, we wondered whether the defect could be complemented by the expression of the wild-type *eep* locus in *trans*. As shown in Fig. 4, the Δ*eep* endocarditis defect was fully rescued when the locus was expressed under the control of a nisin-inducible promoter on a plasmid. The mean weight (± standard deviation) of vegetations formed by the complemented strain was 32.1 ± 35.3 mg (*P* value of 0.027 compared to the Δ*eep* strain). Only 2% of the cells retained the complementation plasmid at the end of the experiment due to the lack of antibiotic selection to maintain the plasmid. In addition, cells were not exposed to the inducing agent during infection, so Eep levels would have been the most abundant at the time of inoculation. The RIVET clone encoding the promoter for the *eep* locus was isolated from the subdermal abscess model at 8 h postinoculation (see Table S2 in the supplemental material), meaning that the promoter was activated within the first several hours of infection. Taken together, these data suggest that the role of Eep in endocarditis occurs during the early stages of valve infection.

**Characterization of *in vitro* biofilm formation by Δ*proB*, Δ*ebrA*, and Δ*eep* strains.** Biofilm formation by OG1RF and the Δ*proB*, Δ*ebrA*, and Δ*eep* strains was evaluated at the 4- and 24-h time points by using *in vitro* biofilm assays that examined the total biomass or recovery of viable cells. No defects in biofilm formation were detected among any of the strains at 4 or 24 h in the three assays (see Fig. S1 in the supplemental material).

The significant endocarditis attenuation demonstrated by the Δ*eep* strain led us to use immunofluorescence microscopy to further characterize biofilms formed by this strain. A striking morphological difference between the mutant and wild-type strains was observed for *E. faecalis in vitro* biofilms grown for 6 h (Fig. 5). By use of a lectin conjugate that localizes primarily to the bacterial cell envelope, the Δ*eep* strain biofilms were found to be composed largely of small cellular aggregates; such structures were not observed in OG1RF biofilms at the same time point. This phenotypic difference could be seen even under a low magnification (×200) (Fig. 5A and B). Quantitative COMSTAT2 analysis of the biomass was consistent with the fluorescent micrographs (see Table S4 in the supplemental material). While the average biomass was only slightly elevated in the mutant strain (~23% higher), the range of variation between samples was much greater for the Δ*eep* strain biofilms.

## DISCUSSION

The emergence of multidrug-resistant enterococcal infections in hospitalized and immunocompromised individuals in recent years emphasizes the importance of elucidating the genetic basis of enterococcal pathogenicity. The expression of virulence factors in *E. faecalis*, whether encoded on mobile genetic elements in select strains or found in the chromosomes of all strains, is likely part of a larger physiological adaptation that *E. faecalis* cells undergo when occupying a niche as a pathogen. Here we report the results of a genome-level analysis using RIVET to identify genetic factors that are upregulated during the course of *E. faecalis* subdermal abscess infection. The use of the plasmid- and pathogenicity island-free *E. faecalis* strain OG1RF in this study allowed us to gain insights into gene expression from the *E. faecalis* core genome during the establishment of infection. In addition, by comparing the results of RIVET screens carried out with the subdermal abscess infection model and in *in vitro* biofilms (4), we were able to attribute functions for *in vivo* growth and virulence to two genes in *E. faecalis* that were not previously associated with the infection process (Fig. 4).

An advantage that RIVET methodology provides is the ability to detect heterogeneous gene expression among cells in sampled populations. We identified many *in vivo*-activated promoters with the RIVET screen (Fig. 2 and see Tables S2 and S3 in the supplemental material) across multiple time points in the subdermal infection model. Those genes that are transiently expressed or are highly expressed in only a minor subpopulation of the enterococci in the host would not have been detected with other types of gene expression techniques (e.g., microarray analysis). The RIVET screen also permitted the sampling of multiple locations in the model, including the inner surface of an explanted subdermal chamber. Only one *in vivo*-activated promoter from a surface-associated clone was found to overlap with biofilm growth-associated genes (Table 2), suggesting that many of the genes listed

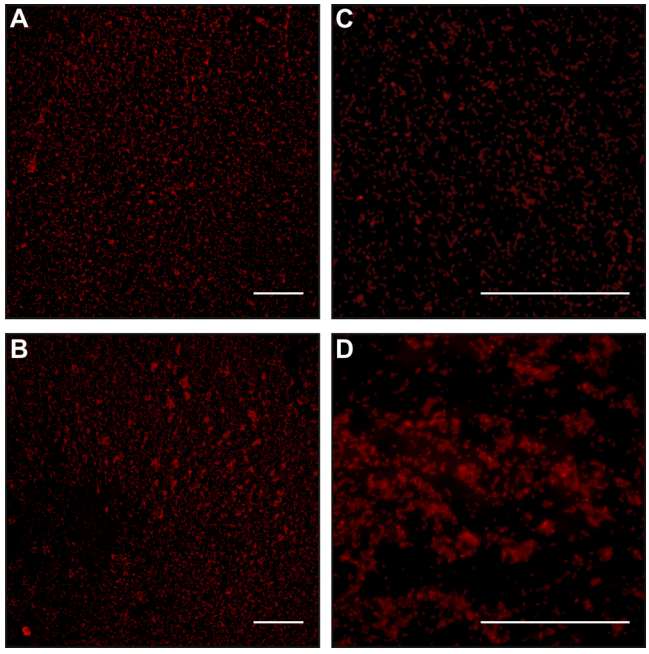


**FIG 5** Fluorescent micrographs of OG1RF (A and C) and Δ*eep* strain (B and D) biofilms at 6 h postinoculation. Biofilms were grown on Aclar fluoropolymer coupons in tryptic soy broth without added dextrose, washed, and stained with wheat germ agglutinin conjugated to Alexa Fluor 594 as described in Materials and Methods. Representative images acquired at magnifications of ×200 (A and B) and ×600 (C and D) are shown. Scale bars, 20 μm.

in Table 2 may be important for the adaptation of *E. faecalis* to alternate growth conditions besides biofilms.

We encountered difficulty in isolating resolved clones from the 24-h time point due to the high levels of background growth of unresolved clones on the counterselective agent 5FU. In *E. coli* and *Bacillus subtilis*, uracil uptake and transport are hindered by elevated levels of ppGpp associated with a stringent response (6, 40). We have observed by microarray analysis that OG1RF cells in the subdermal abscess model activate a stringent response by 8 h postinoculation (Frank and Dunny, unpublished). Thus, the apparent decrease in 5FU toxicity at 24 h postinoculation may be a result of the physiological state of the bacteria in the subdermal abscess environment.

Two other genome-wide screens for *E. faecalis* genes that contribute to growth and virulence in a host have been performed. A Cre recombinase-based RIVET method for a plasmid-free derivative of *E. faecalis* V583 was recently developed (27). Over 60 activated genes were collectively identified by this method in screens performed in mouse models of peritonitis and bacteremia. Two of the genes, EF0106 (carbamate kinase) and EF2987 (a conserved hypothetical protein), were found in our RIVET screen. Those authors also screened for *in vivo*-activated promoters in *Galleria mellonella* larvae; zero of the four *in vivo*-activated promoters identified were found in our RIVET screen. A different group evaluated 540 OG1RF Tn*917* transposon insertion mutants for their abilities to kill the nematode *Caenorhabditis elegans* (34). Twenty-three of the insertion mutants were attenuated in the killing of *C. elegans*, with five of the mutants also showing attenuation in a mouse model of peritonitis. None of these genes were found to be upregulated in our RIVET data sets. The complete lack of overlap in the data collected from the *C. elegans* and *G. mellonella* models with our data may be due to the use of nonmammalian hosts, suggesting that such models may not be ideal for the identification of genes involved in mammalian adaptation. The differences in strains, mammalian hosts, and infection models used in our study compared to those used in the mammalian Cre recombinase-based RIVET screens may have all contributed to the fact that there was little overlap observed between the two studies. Regardless, further investigation of the two overlapping *in vivo*-expressed genes is warranted, as their functions may be critical for *E. faecalis* adaptation in mammalian environments.

The prevalence of small regulatory RNAs, including antisense RNAs, in bacteria has recently become apparent (59). The expression of bacterial antisense RNAs during infection has been noted in studies that employed tiling arrays (61), IVET (54, 55), and RIVET (11, 42, 43, 56). Approximately 1,000 antisense transcripts have been identified in *E. coli*; many of the antisense transcripts initiated from a nucleotide located within the open reading frame encoded on the sense strand (20). Five antisense RIVET clones were isolated in our previously reported *in vitro* biofilm RIVET screen (4), and antisense clones were apparently found in the *E. faecalis* Cre recombinase-based RIVET screen, although those authors did not report any information about the identities of the putative antisense promoters (27). Over one-third of the RIVET clones in this study had genomic DNA inserts oriented upstream of the recombinase such that expression from the putative promoters would result in the production of antisense transcripts (see Table S3 in the supplemental material). While it seems unlikely that all of these clones contain legitimate promoters, we used RT-PCR to confirm the *in vitro* and *in vivo* expressions of three antisense RNAs predicted by the antisense RIVET clones (Fig. 3). These data serve as the first demonstration of antisense transcripts generated from the *E. faecalis* chromosome during growth in a mammalian host. A recent study described the presence of several noncoding and antisense RNA species in *E. faecalis* (25). Those authors detected transcripts predicted by two of our RIVET antisense clones (RIVET antisense clones EF0867 and EF3260), providing further confirmation of the RIVET screen's role in predicting antisense RNAs in *E. faecalis*. Our data suggest that genome-wide antisense RNA expression occurs in *E. faecalis* during *in vivo* growth. In addition, this finding suggests that RIVET may be a useful method for the identification and characterization of the expression of noncoding RNAs.

When we tested whether the genes *proB* and *ebrA* (Table 2) were important for either biofilm formation or endocarditis, we found that OG1RF strains lacking either gene did not show any biofilm formation defects (see Fig. S1 in the supplemental material) and that the Δ*proB* strain, but not the Δ*ebrA* strain, was slightly attenuated in endocarditis (Fig. 4). These data emphasize that *in vitro* biofilm formation and endocarditis development are not necessarily correlated. The work presented here is the first report of a role for *proB*, encoding glutamate 5-kinase, in *E. faecalis in vivo* growth. Our finding differs from those reported previously for *Listeria monocytogenes*, where a *proBA* mutant was shown to be as virulent as the wild-type strain in mouse intraperitoneal and peroral infections (57). Previously reported work showed that *ebrA* is upregulated in biofilm cells and that lower numbers of cells of a strain lacking *ebrA* were recovered from biofilms grown on cellulose membranes than wild-type cells (4). A similar effect was not observed in the present study, in which biofilms were grown on coupons made of the fluoropolymer Aclar. This difference may be attributable to the chemical differences in the substrates on which the biofilms were grown.

We have shown here that the membrane protease Eep, which was transcriptionally activated early during the subdermal abscess infection (see Table S2 in the supplemental material), was required for effective *E. faecalis* virulence in an endocarditis model (Fig. 4) and that it affects cellular distribution during early biofilm formation *in vitro* (Fig. 5). Notably, the Δ*eep* strain produces the greatest decrease in endocarditis virulence of any single-gene knockout that we have tested to date (approximately a dozen genes tested) (Fig. 4) (Frank and Dunny, unpublished). In *E. faecalis*, Eep is known to be involved in the proteolytic processing of several sex pheromone peptides that are located within the signal sequences of lipoproteins (1, 2, 13, 18); mature pheromones extracellularly induce conjugation in a class of large pheromone-responsive conjugative plasmids (e.g., pCF10 and pAD1) (17, 22). The sex pheromone-related function of Eep was characterized using cells grown in routine laboratory medium (2, 13), indicating that *eep* is expressed *in vitro* to some degree. Despite pregrowing the RIVET library inoculum to eliminate *in vitro*-expressed promoters, RIVET plasmids carrying the *eep* locus were isolated *in vivo* in this study and in biofilms (4). It is conceivable that a very low level of *eep* transcription, or transcription in a small subset of cells in a population, during growth in laboratory medium generates sufficient Eep enzymatic activity for the processing of the very low levels of pheromones that are secreted (9, 39). Such cells may not have been eliminated during the *in vitro* pregrowth because the selection agent, kanamycin, is not bactericidal against most enterococcal strains, even at the high levels used in this study. Since the biofilm and *in vivo* RIVET screens were carried out using a plasmid-free version of OG1RF, our data provide the first description of a function for Eep in *E. faecalis* that does not directly involve the processing of signaling molecules for

pheromone-inducible conjugative plasmids. The observations that the level of *eep* locus transcription is increased during biofilm formation and under *in vivo* growth conditions and that the Δ*eep* mutant has altered phenotypes in developing biofilms and causing endocarditis suggest that the protease has broader functions.

Eep belongs to the site 2 protease class of intramembrane proteases found in organisms ranging from bacteria to humans (62). Bacterial site 2 proteases have functions in both physiology and pathogenesis (35, 62); examples of these functions include sporulation in *Bacillus subtilis* (49), cell polarity in *Caulobacter* spp. (14), alginate production in *Pseudomonas aeruginosa* (47, 65), and toxin expression in *Vibrio cholerae* (36). A function for site 2 proteases in pathogenesis is consistent with our observation that an Eep-deficient strain was severely attenuated in forming vegetations on damaged heart valves. One hypothesis for the *in vivo* function of Eep is that it has a more general role in the processing of *E. faecalis* lipoproteins beyond the generation of mature conjugative pheromones (2, 13). A similar function has been attributed to an Eep homolog found in the bovine mastitis pathogen *Streptococcus uberis* (19). Alternatively, Eep may act as a structural component of the *E. faecalis* cell envelope or process other types of peptide signals that are important during biofilm growth and infection.

Finally, the fluorescent micrographs shown in Fig. 5 demonstrate that the loss of Eep leads to a visible phenotype in early *in vitro* biofilms. The lack of Eep shifts the cellular distribution from being generally uniform (Fig. 5A and C) to a discrete clustering phenotype (Fig. 5B and D). In addition, the diffuse extracellular labeling by the WGA lectin (used here primarily to visualize the cell envelope) also suggests that under these conditions, mutant biofilms may produce either more extracellular matrix or a matrix with higher levels of polysaccharides comprised of *N*-acetylglucosamine or sialic acid residues. Deciphering whether the biofilm cell distribution phenotype shown in Fig. 5 is specifically caused by the loss of Eep and addressing the relationship between these *in vitro* observations and the *in vivo* biofilm results are avenues of current investigation.

In conclusion, we have identified genes in the core genome of *E. faecalis* OG1RF that contribute to the ability of this important nosocomial pathogen to adapt to and survive in a mammalian host. These data revealed two significant and novel observations: (i) the membrane metalloprotease Eep is a major virulence determinant in *E. faecalis*, and (ii) multiple antisense RNA transcripts are expressed in *E. faecalis* during infection. This work also illustrates how RIVET screens provide useful information about the temporal activation of genes in a pathogen during infection. In addition, we have shown how the application of a single genetic technique under two different conditions led to the identification and confirmation of a new virulence determinant. The data presented here will provide a foundation for future studies that should begin to unravel the sensing and regulatory pathways that *E. faecalis* uses to adapt to and survive in its surroundings in a host.

## ACKNOWLEDGMENTS

We gratefully acknowledge Christopher Kristich and Katie Ballering for their advice on setting up and conducting the RIVET experiments and Petra Kohler, Olivia Chuang-Smith, Jillian Vocke, and Adam Spaulding for their instrumental roles in performing the endocarditis experiments.

This work was carried out in part using computing resources provided by the University of Minnesota Supercomputing Institute. Genome annotation was carried out with RAST, which is supported in part by the National Institute of Allergy and Infectious Diseases (NIAID), National Institutes of Health, Department of Health and Human Services, under contract number HHSN266200400042C. This research was supported by award number R01AI58134 from the National Institute of Allergy and Infectious Diseases to G.M.D. A.M.T.B. received additional support from NIH medical scientist training grant number T32GM008244. K.L.F. was supported by award number F32AI082881 from the National Institute of Allergy and Infectious Diseases, award number T32DE007288 from the National Institute of Dental and Craniofacial Research, and award number 10POST3290026 from the American Heart Association.

The content is solely the responsibility of the authors and does not necessarily represent the official views of the National Institute of Allergy and Infectious Diseases, the National Institute of General Medical Sciences, the National Institute of Dental and Craniofacial Research, the National Institutes of Health, or the American Heart Association. The funders had no role in study design, data collection and analysis, decision to publish, or preparation of the manuscript.

## REFERENCES

1. **An FY, Clewell DB.** 2002. Identification of the cAD1 sex pheromone precursor in *Enterococcus faecalis.* J. Bacteriol. **184**:1880–1887.
2. **An FY, Sulavik MC, Clewell DB.** 1999. Identification and characterization of a determinant (*eep*) on the *Enterococcus faecalis* chromosome that is involved in production of the peptide sex pheromone cAD1. J. Bacteriol. **181**:5915–5921.
3. **Aziz RK, et al.** 2008. The RAST server: rapid annotations using subsystems technology. BMC Genomics **9**:75.
4. **Ballering KS, et al.** 2009. Functional genomics of *Enterococcus faecalis*: multiple novel genetic determinants for biofilm formation in the core genome. J. Bacteriol. **191**:2806–2814.
5. **Bayer AS, Coulter SN, Stover CK, Schwan WR.** 1999. Impact of the high-affinity proline permease gene (*putP*) on the virulence of *Staphylococcus aureus* in experimental endocarditis. Infect. Immun. **67**:740–744.
6. **Beaman TC, et al.** 1983. Specificity and control of uptake of purines and other compounds in *Bacillus subtilis.* J. Bacteriol. **156**:1107–1117.
7. **Bourgogne A, et al.** 2008. Large scale variation in *Enterococcus faecalis* illustrated by the genome analysis of strain OG1RF. Genome Biol. **9**:R110.
8. **Bryan EM, Bae T, Kleerebezem M, Dunny GM.** 2000. Improved vectors for nisin-controlled expression in gram-positive bacteria. Plasmid **44**: 183–190.
9. **Buttaro BA, Antiporta MH, Dunny GM.** 2000. Cell-associated pheromone peptide (cCF10) production and pheromone inhibition in *Enterococcus faecalis.* J. Bacteriol. **182**:4926–4933.
10. **Camilli A, Beattie DT, Mekalanos JJ.** 1994. Use of genetic recombination as a reporter of gene expression. Proc. Natl. Acad. Sci. U. S. A. **91**:2634–2638.
11. **Camilli A, Mekalanos JJ.** 1995. Use of recombinase gene fusions to identify *Vibrio cholerae* genes induced during infection. Mol. Microbiol. **18**: 671–683.
12. **Castillo AR, Woodruff AJ, Connolly LE, Sause WE, Ottemann KM.** 2008. Recombination-based *in vivo* expression technology identifies *Helicobacter pylori* genes important for host colonization. Infect. Immun. **76**: 5632–5644.
13. **Chandler JR, Dunny GM.** 2008. Characterization of the sequence specificity determinants required for processing and control of sex pheromone by the intramembrane protease Eep and the plasmid-encoded protein PrgY. J. Bacteriol. **190**:1172–1183.
14. **Chen JC, Viollier PH, Shapiro L.** 2005. A membrane metalloprotease participates in the sequential degradation of a *Caulobacter* polarity determinant. Mol. Microbiol. **55**:1085–1103.
15. **Chiang SL, Mekalanos JJ, Holden DW.** 1999. *In vivo* genetic analysis of bacterial virulence. Annu. Rev. Microbiol. **53**:129–154.
16. **Chuang ON, et al.** 2009. Multiple functional domains of *Enterococcus faecalis* aggregation substance Asc10 contribute to endocarditis virulence. Infect. Immun. **77**:539–548.
17. **Clewell DB.** 2007. Properties of *Enterococcus faecalis* plasmid pAD1, a member of a widely disseminated family of pheromone-responding, conjugative, virulence elements encoding cytolysin. Plasmid **58**:205–227.
18. **Clewell DB, An FY, Flannagan SE, Antiporta M, Dunny GM.** 2000. Enterococcal sex pheromone precursors are part of signal sequences for surface lipoproteins. Mol. Microbiol. **35**:246–247.

19. **Denham EL, Ward PN, Leigh JA.** 2008. Lipoprotein signal peptides are processed by Lsp and Eep of *Streptococcus uberis.* J. Bacteriol. **190**:4641–4647.
20. **Dornenburg JE, DeVita AM, Palumbo MJ, Wade JT.** 2010. Widespread antisense transcription in *Escherichia coli.* mBio **1**:e00024-10. doi:10.1128/mBio.00024-10.
21. **Dunny GM, Brown BL, Clewell DB.** 1978. Induced cell aggregation and mating in *Streptococcus faecalis*: evidence for a bacterial sex pheromone. Proc. Natl. Acad. Sci. U. S. A. **75**:3479–3483.
22. **Dunny GM, Johnson CM.** 2011. Regulatory circuits controlling enterococcal conjugation: lessons for functional genomics. Curr. Opin. Microbiol. **14**:174–180.
23. **Facklam RR, Carvalho M, Teixeira LM.** 2002. History, taxonomy, biochemical characteristics, and antibiotic susceptibility testing of enterococci, p 1–54. *In* Gilmore MS, et al (ed), The enterococci: pathogenesis, molecular biology, and antibiotic resistance. ASM Press, Washington, DC.
24. **Fisher K, Phillips C.** 2009. The ecology, epidemiology and virulence of *Enterococcus.* Microbiology **155**:1749–1757.
25. **Fouquier d'Herouel A, et al.** 2011. A simple and efficient method to search for selected primary transcripts: non-coding and antisense RNAs in the human pathogen *Enterococcus faecalis.* Nucleic Acids Res. **39**:e46.
26. **Graham MR, et al.** 2006. Analysis of the transcriptome of group A *Streptococcus* in mouse soft tissue infection. Am. J. Pathol. **169**:927–942.
27. **Hanin A, et al.** 2010. Screening of *in vivo* activated genes in *Enterococcus faecalis* during insect and mouse infections and growth in urine. PLoS One **5**:e11879.
28. **Heydorn A, et al.** 2000. Quantification of biofilm structures by the novel computer program COMSTAT. Microbiology **146**(Pt 10):2395–2407.
29. **Kristich CJ, Chandler JR, Dunny GM.** 2007. Development of a host-genotype-independent counterselectable marker and a high-frequency conjugative delivery system and their use in genetic analysis of *Enterococcus faecalis.* Plasmid **57**:131–144.
30. **Kristich CJ, Li YH, Cvitkovitch DG, Dunny GM.** 2004. Esp-independent biofilm formation by *Enterococcus faecalis.* J. Bacteriol. **186**:154–163.
31. **Kristich CJ, et al.** 2008. Development and use of an efficient system for random *mariner* transposon mutagenesis to identify novel genetic determinants of biofilm formation in the core *Enterococcus faecalis* genome. Appl. Environ. Microbiol. **74**:3377–3386.
32. **Liang FT, Nelson FK, Fikrig E.** 2002. Molecular adaptation of *Borrelia burgdorferi* in the murine host. J. Exp. Med. **196**:275–280.
33. **Lowe AM, Beattie DT, Deresiewicz RL.** 1998. Identification of novel staphylococcal virulence genes by *in vivo* expression technology. Mol. Microbiol. **27**:967–976.
34. **Maadani A, Fox KA, Mylonakis E, Garsin DA.** 2007. *Enterococcus faecalis* mutations affecting virulence in the *Caenorhabditis elegans* model host. Infect. Immun. **75**:2634–2637.
35. **Makinoshima H, Glickman MS.** 2006. Site-2 proteases in prokaryotes: regulated intramembrane proteolysis expands to microbial pathogenesis. Microbes Infect. **8**:1882–1888.
36. **Matson JS, DiRita VJ.** 2005. Degradation of the membrane-localized virulence activator TcpP by the YaeL protease in *Vibrio cholerae.* Proc. Natl. Acad. Sci. U. S. A. **102**:16403–16408.
37. **Mohamed JA, Huang DB.** 2007. Biofilm formation by enterococci. J. Med. Microbiol. **56**:1581–1588.
38. **Mutnick AH, Biedenbach DJ, Jones RN.** 2003. Geographic variations and trends in antimicrobial resistance among *Enterococcus faecalis* and *Enterococcus faecium* in the SENTRY Antimicrobial Surveillance Program (1997–2000). Diagn. Microbiol. Infect. Dis. **46**:63–68.
39. **Nakayama J, Ruhfel RE, Dunny GM, Isogai A, Suzuki A.** 1994. The *prgQ* gene of the *Enterococcus faecalis* tetracycline resistance plasmid pCF10 encodes a peptide inhibitor, iCF10. J. Bacteriol. **176**:7405–7408.
40. **Neuhard J.** 1983. Utilization of preformed pyrimidine bases and nucleosides, p 95–148. *In* Munch-Petersen A (ed), Metabolism of nucleotides, nucleosides, and nucleobases in microorganisms. Academic Press, Inc, New York, NY.
41. **Orihuela CJ, et al.** 2004. Microarray analysis of pneumococcal gene expression during invasive disease. Infect. Immun. **72**:5582–5596.
42. **Osorio CG, Camilli A.** 2003. Hidden dimensions of *Vibrio cholerae* pathogenesis. ASM News **69**:396–401.
43. **Osorio CG, et al.** 2005. Second-generation recombination-based *in vivo* expression technology for large-scale screening for *Vibrio cholerae* genes induced during infection of the mouse small intestine. Infect. Immun. **73**:972–980.
44. **Paulsen IT, et al.** 2003. Role of mobile DNA in the evolution of vancomycin-resistant *Enterococcus faecalis.* Science **299**:2071–2074.
45. **Pfaffl MW.** 2001. A new mathematical model for relative quantification in real-time RT-PCR. Nucleic Acids Res. **29**:e45.
46. **Pfaller MA, et al.** 1999. Survey of blood stream infections attributable to Gram-positive cocci: frequency of occurrence and antimicrobial susceptibility of isolates collected in 1997 in the United States, Canada, and Latin America from the SENTRY Antimicrobial Surveillance Program. SENTRY Participants Group. Diagn. Microbiol. Infect. Dis. **33**:283–297.
47. **Qiu D, Eisinger VM, Rowen DW, Yu HD.** 2007. Regulated proteolysis controls mucoid conversion in *Pseudomonas aeruginosa.* Proc. Natl. Acad. Sci. U. S. A. **104**:8107–8112.
48. **Roggiani M, Schlievert PM.** 2000. Purification of streptococcal pyrogenic exotoxin A, p 59–66. *In* Evans TJ (ed), Septic shock methods and protocols, vol 36. Humana Press, Totowa, NJ.
49. **Rudner DZ, Fawcett P, Losick R.** 1999. A family of membrane-embedded metalloproteases involved in regulated proteolysis of membrane-associated transcription factors. Proc. Natl. Acad. Sci. U. S. A. **96**:14765–14770.
50. **Schlievert PM.** 2007. Chitosan malate inhibits growth and exotoxin production of toxic shock syndrome-inducing *Staphylococcus aureus* strains and group A streptococci. Antimicrob. Agents Chemother. **51**:3056–3062.
51. **Schwan WR, et al.** 1998. Identification and characterization of the PutP proline permease that contributes to in vivo survival of *Staphylococcus aureus* in animal models. Infect. Immun. **66**:567–572.
52. **Scott DF, Kling JM, Kirkland JJ, Best GK.** 1983. Characterization of *Staphylococcus aureus* isolates from patients with toxic shock syndrome, using polyethylene infection chambers in rabbits. Infect. Immun. **39**:383–387.
53. **Shepard BD, Gilmore MS.** 2002. Differential expression of virulence-related genes in *Enterococcus faecalis* in response to biological cues in serum and urine. Infect. Immun. **70**:4344–4352.
54. **Silby MW, Levy SB.** 2008. Overlapping protein-encoding genes in *Pseudomonas fluorescens* Pf0-1. PLoS Genet. **4**:e1000094.
55. **Silby MW, Levy SB.** 2004. Use of *in vivo* expression technology to identify genes important in growth and survival of *Pseudomonas fluorescens* Pf0-1 in soil: discovery of expressed sequences with novel genetic organization. J. Bacteriol. **186**:7411–7419.
56. **Slauch JM, Camilli A.** 2000. IVET and RIVET: use of gene fusions to identify bacterial virulence factors specifically induced in host tissues. Methods Enzymol. **326**:73–96.
57. **Sleator RD, Gahan CG, Hill C.** 2001. Identification and disruption of the *proBA* locus in *Listeria monocytogenes*: role of proline biosynthesis in salt tolerance and murine infection. Appl. Environ. Microbiol. **67**:2571–2577.
58. **Talaat AM, Lyons R, Howard ST, Johnston SA.** 2004. The temporal expression profile of *Mycobacterium tuberculosis* infection in mice. Proc. Natl. Acad. Sci. U. S. A. **101**:4602–4607.
59. **Thomason MK, Storz G.** 2010. Bacterial antisense RNAs: how many are there, and what are they doing? Annu. Rev. Genet. **44**:167–188.
60. **Tight RR, Prior RB, Perkins RL, Rotilie CA.** 1975. Fluid and penicillin G dynamics in polyethylene chambers implanted subcutaneously in rabbits. Antimicrob. Agents Chemother. **8**:495–497.
61. **Toledo-Arana A, et al.** 2009. The *Listeria* transcriptional landscape from saprophytism to virulence. Nature **459**:950–956.
62. **Urban S.** 2009. Making the cut: central roles of intramembrane proteolysis in pathogenic microorganisms. Nat. Rev. Microbiol. **7**:411–423.
63. **Vadyvaloo V, Jarrett C, Sturdevant DE, Sebbane F, Hinnebusch BJ.** 2010. Transit through the flea vector induces a pretransmission innate immunity resistance phenotype in *Yersinia pestis.* PLoS Pathog. **6**:e1000783.
64. **Vebø HC, Snipen L, Nes IF, Brede DA.** 2009. The transcriptome of the nosocomial pathogen *Enterococcus faecalis* V583 reveals adaptive responses to growth in blood. PLoS One **4**:e7660.
65. **Wood LF, Ohman DE.** 2009. Use of cell wall stress to characterize sigma 22 (AlgT/U) activation by regulated proteolysis and its regulon in *Pseudomonas aeruginosa.* Mol. Microbiol. **72**:183–201.
66. **Xu Q, Dziejman M, Mekalanos JJ.** 2003. Determination of the transcriptome of *Vibrio cholerae* during intraintestinal growth and midexponential phase *in vitro.* Proc. Natl. Acad. Sci. U. S. A. **100**:1286–1291.
67. **Yarwood JM, McCormick JK, Paustian ML, Kapur V, Schlievert PM.** 2002. Repression of the *Staphylococcus aureus* accessory gene regulator in serum and *in vivo.* J. Bacteriol. **184**:1095–1101.